



Theoretical Modelling of Acoustical Measurement Accuracy for Swath Bathymetric Sonars

By Xavier Lurton, Ifremer - Service Acoustique et Sismique, France

Multibeam echosounders and bathymetric side-scan sonars are nowadays widely used for seafloor topographic mapping. Depending on the measurement angle sector and on the sonar array structure, various methods are usable to estimate time-angle pairs needed to determine sounding point positions. Distinctions are to be made between methods based on either signal amplitude or phase; and between measurements at either given time or angle; this leads to define four main methods, covering most of bathymetry systems available today (maximum amplitude instant, phase difference direction, zero-phase difference instant, maximum amplitude direction). In this paper, the principles of these four approaches are presented, and their respective measurement accuracy is evaluated as a function of the signal-to-noise ratio. The averaging over a

number of samples is considered; also the specificity of measurements close to the vertical is discussed. An application example is finally presented.

Introduction

Most seafloor topographic mapping surveys are carried out using specialised bathymetric sonars. Limited for a long time to vertical sounding carried out by single-beam sounders, bathymetric sonars used today mainly work in oblique incidence. Installed under the hull of a ship or on an underwater vehicle, a swath bathymetry sonar (Figure 1) ensonifies a ground strip, narrow in the alongtrack direction and broad across-track, thanks to one (or two) transmit arrays of large longitudinal dimension. For Bathymetric Side-Scan Sonars (BSSS), the receive arrays are identical to the transmit arrays,

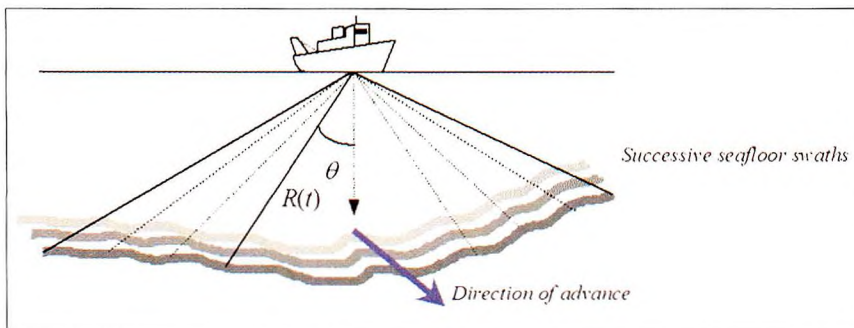


Figure 1: Bathymetric measurement using a swath sonar: each sounding point along the across-track ensonified strip is defined by measurements of angle θ and oblique range R given by the two-way travel time t

and do not provide additional angular filtering. For MultiBeam EchoSounders (MBES), echoes are received inside a vertical fan of narrow beams, formed using an ad hoc array.

In all cases, the received backscattered echo is recorded as a function of time. After the complete reception of an echo, the sonar emits a new signal that covers a seafloor strip shifted due to vessel advance. The seafloor echoes are used on the one hand to perform bathymetric measurements, and on the other hand to build the sonar imagery from the bottom reflectivity; only the first topic is considered in this paper.

Every sounding measurement by a bathymetric sonar is based on the joint estimate of two characteristics (range and angle of arrival) of echoes; these allow one to locate the impact point positions on the bottom relative to the sonar, taking into consideration the propagation characteristics. These points are then positioned geographically starting from measurements of navigation and vessel attitude with respect to the sonar. This paper will examine only the first part of this series of operations, i.e. the processing of the acoustic signals for the (range, angle) estimation. The detailed analysis of the other causes of errors (platform attitude, refraction due to sound speed, etc.) and their influence are detailed in [Hare et al., 1995].

Since the oblique range is given by the two-way propagation time t (ideally $R(t) = ct/2$ for a medium with constant sound velocity c), its estimation will be, in the following, equivalently considered in the time domain.

Two categories of (time, angle) measurement methods may be distinguished:

- Arrival time estimation, for fixed observation angles
- Arrival angle estimation, as a function of time in reception

Each one of the two approaches above can be applied to either amplitude or phase criteria of the received signal; this leads therefore to four methods; every current bathymetric sonar uses one or two of these. We will refer to them in the remainder of this paper as:

- Maximum Amplitude Instant (MAI): estimation of the instant corresponding to the maximum energy of the received temporal signal inside a beam formed in a given direction

- Zero-phase Difference Instant (ZDI): estimation of the instant corresponding to null phase difference between two beams formed in a given direction
- Phase Difference Direction (PDD): estimation of the arrival angle at a given instant, from the phase difference between the time signals on two sensors
- Maximum Amplitude Direction (MAD): estimation of the angle corresponding to the maximum energy among a fan of beams considered at a given instant

In all cases, spatial processing is necessary to perform angle measurements, which are implemented either starting from a beamforming array (MAI, MAD), or starting from a dephasing measurement between two simple receivers (PDD), or else by mixing both approaches (ZDI). The systems considered here are MBES (carrying out the measurement of bathymetry at the output of many formed beams) and BSSS (working on the phase difference between signals received on two, or more, receiving arrays).

The fundamentals of these various methods of array and signal processing are classical (they may be found e.g. in Burdic's textbook [Burdic, 1984]). They have been applied progressively to the various generations of swath bathymetric sonars (see e.g. review papers [de Moustier, 1988] and [de Moustier, 1993]). For multibeam echosounders, MAI alone was used in the pioneer SeaBeam system ([Renard & Allenou, 1979]). In order to get wider swath widths, MAI was later completed by either ZDI ([Pohner, 1987]) or MAD ([Satriano et al., 1991]), depending on manufacturers. On the other hand, sidescan sonars began to be equipped with PDD interferometers in the early 1980s ([Blackington, 1986], [Denbigh, 1989]). Theoretical elements and comparisons between these sonar processing methods (possibly outside the bathymetry measurement context) may also be found in [Quazi, 1981], [Billon, 1987] or [Leclerc, 1994].

In the present paper, after defining the geometrical configuration and limiting the scope of our study, we examine in the main section the four methods of measurement. In each case, expressions of angular and bathymetric errors are proposed according to Signal to Noise Ratio (SNR) and sonar characteristics. The variance reduction due to averaging of successive samples is examined, as

well as the particular problems raised by measurements at incidence angles close to the vertical. An example of application to a typical sonar configuration is also presented.

General Presentation

Measurement Configuration

The geometrical configuration is shown in Figure 2. The bottom is assumed to be flat and horizontal, with homogeneous characteristics; acoustical backscatter is caused only by the $z=0$ interface. The sonar system is assumed to have a narrow directivity pattern in the y direction (normal to the measurement plane xz), so that propagation and backscatter are confined to the vertical plane xz . The receiving array, situated at altitude H above the seafloor, is rectangular with dimensions L in the xz plane and w in the xy plane (not shown in Figure 2); the array is tilted at an angle ψ with respect to the horizontal. At the time of measurement, the direction of the (supposed rectilinear) signal trajectory makes an angle θ with the bottom, and $\gamma = \theta - \psi$ with respect to the axis normal to the array length.

Joint estimation, in reception, of the backscattered wave angle θ together with the time of flight t allows computation of the impact point position. For example, assuming propagation with constant sound speed c , the instantaneous oblique range is $R = \frac{ct}{2}$, and one obtains for the impact point coordinates

$$D = \frac{ct}{2} \sin \theta \text{ and } H = \frac{ct}{2} \cos \theta$$

The depth relative error is therefore linked to the measurement errors in time and angle by:

$$\frac{\delta H}{H} = \frac{\delta t}{t} + \tan \theta \cdot \delta \theta \tag{1}$$

Hypotheses on Signal and Noise

In the following, a received signal of average power $\langle P \rangle$ is superimposed on a white Gaussian noise, in the signal frequency band, spatially isotropic, with average power $\langle n \rangle$; the input SNR is therefore

$$d_0 = \frac{\langle P \rangle}{\langle n \rangle}$$

Considering that the estimation of parameters is carried out after adapted filtering and receiver array processing, the output SNR to consider becomes:

$$d = G_D d_0 \tag{2}$$

where G_D is the array directivity index. In the ideal case of a rectangular array of dimensions (w, L) , consisting of omnidirectional sensors summed without weighting, and forming a beam in the direction γ , the array directivity index is approximated by:

$$G_D \approx \frac{4\pi Lw \cos \gamma}{\lambda^2} \tag{3}$$

thus depending on the beam steering angle γ .

The signal duration considered here may be, equivalently:

- Either that T of the emitted signal envelope (possibly within -3 dB), in the case of a narrow-band signal
- Or the lobe width (roughly $1/B$) of the autocorrelation function, in the case of a signal modulated with spectral bandwidth B , after a 'pulse compression' processed by an adapted filter

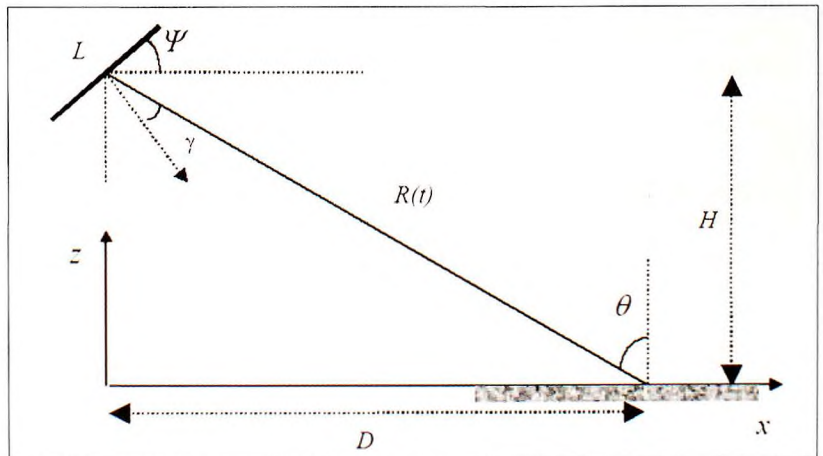


Figure 2: Measurement configuration

The signal received on the array has, in first approximation, a plane wave structure. It is supposed of constant average amplitude (while its instantaneous amplitude may be fluctuating); in other words, inside a beam footprint the average backscatter index is independent of angle, and the transmission loss variations are neglected. In addition, one considers here only the random fluctuations of measurement related to the acoustical SNR, disregarding the other measurement error causes rather leading to estimation biases (array installation geometry, ignorance of the local sound speed profile, etc.).

The noise disturbing measurements may be either additive noise, or degradations related to the structure of the backscattered signal itself.

- Additive noise occurs from acoustical or electrical causes, and intervenes like a random component superimposed on the signal; the effect of this noise upon SNR is reduced by the directivity index of the receiver array [Burdic, 1984], as expressed in (2)
- The effect of *angular decorrelation* is related to the radiation of the echo by a seafloor elementary instantaneous target (delimited by the signal footprint): the array receivers do not perceive this target as a point-like source, but as a scattered sound field with a directivity pattern due to the spatial extent of the signal footprint. This effect can be expressed as a SNR degradation [Jin & Tang, 1996] in:

$$d_{ang} = \frac{\nu}{1 - \nu} \tag{4}$$

with $\nu = \left| \frac{\sin \eta}{\eta} \right|$, and $\eta = \frac{ka}{2H} \Delta x \cos^2 \theta \cos \gamma$,

where k is the acoustic wavenumber and a the spacing between two points of the receiving array. The signal instantaneous spreading Δx on the bottom is:

$$\Delta x = \min \left(\frac{cT}{2 \sin \theta}, \frac{H \Delta \theta}{\cos^2 \theta} \right) \tag{5}$$

given either by the signal duration T or by the angular beam width $\Delta \theta$ inside which detection is carried out. This decorrelation effect, also known in radar as *glint*, corresponds to an angular measurement spreading directly related to the instantaneous target size [Lurton, 2000]

- The effect of *footprint shift* is caused by the

fact that at any given instant the various points of the array do not "see" exactly the same seafloor part [Lurton, 2000]; thus the echo radiated by the non-common scatterers plays the role of disturbing noise. This affects the interferometric measurement of phase difference between separate receivers; in this case the equivalent SNR can be expressed roughly, in oblique incidence, as the ratio between the lengths of the common and non-common parts of the footprint:

$$d_{shf} \approx \frac{cT}{a |\sin \gamma|} - 1 \tag{6}$$

where a is the interferometer spacing¹. Implicitly, d_{shf} tends towards a zero limiting value when the two footprints become completely disjointed. The footprint shift can be corrected if the signal arrival direction is known: in a MBES, each beam nominal angle gives an estimate of γ with a precision sufficient for neglecting this effect. On the other hand the phenomenon is very penalising for BSSS having no *a priori* angular information; one solution, in this case, is to take the first interferometric measurement of γ and then, starting from this estimate, to carry out the preliminary compensation to the final interferometric measurement; another possible solution lies in the use of wide-band modulated signals, in which case the cross-correlation function provides an estimate of time delay between the two receivers giving access to a γ estimate. It should be noted that, even if the footprint shift is compensated, a residual error may subsist, related to the signal time sampling rate. In this case the relationship between common and non-common parts of the footprint becomes:

$$d_{shf} \approx \frac{T}{\tau} - 1 \tag{6a}$$

where τ is the standard deviation of the error due to time sampling period.

To synthesise these various effects, a resulting signal to noise ratio d combines these contributions, assumed independent:

$$\frac{1}{d} = \frac{1}{d_{add}} + \frac{1}{d_{ang}} + \frac{1}{d_{shf}} \tag{7}$$

where d_{add} is the additive SNR, d_{ang} and d_{shf} are the equivalent SNR for angular spreading and shifting footprint. The relative importance of the various terms depends on the system type and the configuration considered.

¹ The corresponding formula in [Lurton, 2000] is erroneous by a factor 2

Beamforming and Array Weighting

In the MBES case, the receiving array forms narrow beams (typically 1° to 2° nominal width) in the xz plane, by dephasing or delaying the signals received on its elementary sensors. Amplitude weighting is applied to limit the effect of the unwanted echoes received by the beam pattern sidelobes, in particular the strong contribution coming from the normal to the bottom (*specular echo*). This method provides a level reduction of the directivity secondary lobes, but at the price of a broadening of the main lobe, and a correlative degradation of the directivity index. For a flat array, the main lobe width (at -3 dB) depends on the array length L and steering angle γ by the approximate relation:

$$\Delta\theta_0(\gamma) \approx 0.88 \frac{\lambda\alpha}{L \cos \gamma} \quad (8)$$

where λ is the wavelength, and α is a corrective coefficient (≥ 1) depending on the particular weighting law. This law differs between sounders, so no general approach will be given here. In the following, the performance of a weighted array will be parameterised by:

- The factor α - widening of the principal lobe (typically 1.2 to 1.4)
- The factor β - degradation of the directivity index (typically 0.6 to 0.8)

Note that, for a rectangular array, $\alpha \approx 1/\beta$ (for a weighting applied to one rectangle side). Refer to e.g. [Harris, 1978] for the detailed definitions and the precise numerical values of these degradation factors.

For a cylindrical array, the beamwidth depends on the active array length considered; it is independent of the steering angle.

Performance of Bathymetric Measurement Methods

Maximum Amplitude Instant

For slightly tilted beams, the MAI method (presumably used in every MBES) basically consists in seeking the maximum amplitude in the temporal signal envelope collected in each formed beam. It is thus a measurement of time of arrival along the beam axis angular direction.

The time signal inside a beam is generated by the emitted signal sweeping the beam footprint on the

bottom. The range difference between the footprint edges, for a beam with width $\Delta\theta_0$ at -3 dB (always considered in the beam vertical plane, and given by (8)), is:

$$\Delta R_0 = \frac{H \sin \theta}{\cos^2 \theta} \Delta\theta_0 \quad (9)$$

from where the temporal spreading (Figure 3) is:

$$\Delta t_0 = \frac{2H \sin \theta}{c \cos^2 \theta} \Delta\theta_0 \quad (10)$$

It should however be noted that, in the case of a beam close to the vertical (typically $\theta < 20^\circ$), this time spreading is usually small. The final time spreading is approximately given by the quadratic summation of the emitted signal duration and the lengthening by angular sweeping, all values considered within -3 dB.

The depth measurement thus corresponds to the arrival time estimate for a fluctuating and noise-added signal of duration $\Theta = \sqrt{T^2 + \Delta t_0^2}$, whose average envelope is a function of the beam pattern, emitted signal shape, and local seafloor roughness; note that at this stage, the sediment interface is considered horizontal, homogeneous and impenetrable to sound waves.

The estimation error for the maximum amplitude instant depends on the actual processing details. A frequently used processing consists in seeking the gravity centre of the echo envelope: the rms error then decreases approximately in proportion with $\frac{\Theta}{\sqrt{N}}$, where N is the number of samples used

in the barycentre computation, and hence depends on the algorithm details. From numerical simulations of a signal envelope fluctuating according to a Rayleigh's law around the average shape of a *sinc* function main lobe (the lobe width being Θ at -3 dB) it may be found (see [Lurton, 2001]) that, if one uses all N signal samples of the average lobe digitised with sampling period T_s , the standard deviation is around $\delta \approx 0.10 \frac{\Theta}{\sqrt{N}} = 0.10 \sqrt{\Theta T_s}$.

This general formulation of a time measurement rms error proportional to the signal duration $\delta = \frac{\xi\Theta}{\sqrt{N}}$ leads to:

$$\delta_{MAI} \approx \frac{\xi}{\sqrt{N}} \left[\left(\frac{2H \sin \theta}{c \cos^2 \theta} \Delta\theta_0 \right)^2 + T^2 \right]^{1/2} \quad (11)$$

The depth measurement relative error is then:

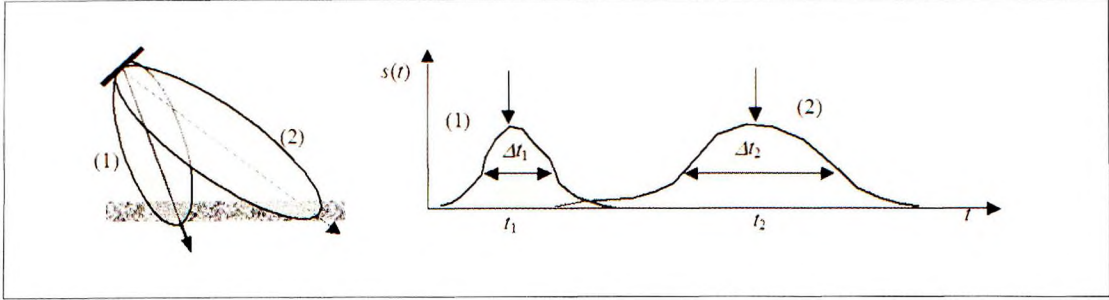


Figure 3: Geometry of two oblique beams of different angles (left) and corresponding signal envelopes used for the estimation of arrival times t_1 and t_2 (right)

$$\frac{\Delta H_{MAL}}{H} \approx \frac{\xi}{\sqrt{N}} \left[(\tan \theta \Delta \theta_0)^2 + \left(\frac{cT}{2H} \cos \theta \right)^2 \right]^{1/2} \quad (12)$$

The measurement error given by (12) is expected to be too optimistic, since time spreading, here defined for an ideal flat seafloor, is clearly underestimated. To be more realistic, the echo envelope model should account for the variations of the seafloor features inside the beam footprint: slope (both alongtrack and across-track), large-scale roughness (hence at a different scale from interface microroughness causing backscattering), penetration inside the sediment volume (echoes raised by buried interfaces and scatterers mixed with the water-sediment interface contribution) and patchiness (horizontal changes of the seafloor type and characteristics). All of these effects cause an extra-spreading related to the relief and sediment variability inside the beam footprint, with a huge variety in configurations making it impossible to model globally. As a first approach, four basic geometrical effects are evoked here (see Figure 4):

- The roughness of an average flat horizontal

interface will cause a time spreading proportional to its peak-to-trough maximum amplitude h (projected at angle θ), hence in $\frac{2h}{c \cdot \cos \theta}$

- be added quadratically inside the brackets of (11)
- The signal penetration inside the seafloor and sediment volume backscattering will create a trail depending upon the frequency and the sediment characteristics (absorption and heterogeneity). Since the absorption coefficient inside soft sediments may be roughly comprised between 0.1 and 0.2 dB/ λ [Hamilton & Bachman, 1982] (or, equivalently, about 0.8 to 1.6 dB/m at 12 kHz), it is readily seen that layers buried at depths of several meters may raise significant echoes blurring the sediment interface detection. This order of magnitude for bathymetry errors makes problematic (along with other causes) the use of low-frequency multibeam echosounders for shallow-water bathymetry applications.
- The across-track average slope ζ_T will modify the effective incident angle θ into $\theta \pm \zeta_T$ inside eq.(9) to (12), the +/- sign depending upon the

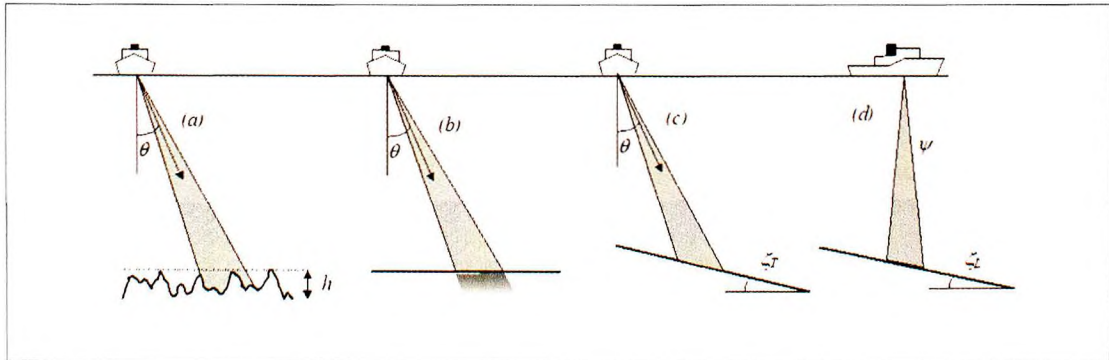


Figure 4: Geometrical approach of echo time spreading for steep beams; effects of roughness (a), sediment penetration (b), across-track slope (c) and along-track slope (d)

slope orientation;

- The alongtrack relative angle ζ_i between the seafloor and the beam fan (due to the average slope and/or non-compensated ship's pitch) will cause a time spreading in $\frac{2H \tan \psi \tan \zeta_i}{\cos \theta}$ (to be

added quadratically inside the brackets of (11)).

Practically, the relative influence of these effects may be strongly dependent upon the seafloor type and the geometrical configuration, precluding the definition of a generic model usable in the present framework.

Moreover, a paramount problem encountered in measuring central beams lies in the elimination of the specular reflected contribution (arriving at

$$t = \frac{2H}{c} \text{ whatever the beam), which may be very}$$

dominant especially at low frequencies. An inaccurate compensation of the specular echo may bias the depth estimates: due to its synchronicity, it tends to circularise the seafloor profile around the central sounding. Its suppression is made very difficult by its proximity in time and angle to the useful backscattered echo.

Away from the vertical, the depth relative error deteriorates according to the $\tan \theta$ term in (12), although the number N of available samples increases with angle θ . Moreover, the above accuracy is obtainable only if the envelope shape of the backscattered pulse is sufficiently short and smooth; thus it is necessary that the bottom structure is flat and homogeneous on the scale of the beam footprint, which may be too strong an assumption at oblique incidences. Note that in actual systems, at oblique and grazing incidences, MAI detection is always replaced by another method.

Phase Difference Direction

The Phase Difference Direction (PDD) method is often used in sonar and radar to locate a target; it consists in measuring, at a given instant, the phase difference between two receiving points, giving a precise estimate of angular direction. In the case of topographic measurement, the cell resolution of the signal on the ground delimits the instantaneous target; a large number of independent measurements can thus be obtained along the swath swept by the signal. This method is employed in BSSS but also in satellite-borne radars for topographic mapping [Maitre, 2001].

Considering the configuration of Figure 5, the phase difference between the signals emanating from M and measured at points A and B , separated by a , is:

$$\Delta \phi_{AB} = k \delta R = ka \sin \gamma \tag{13}$$

where $k = \frac{2\pi}{\lambda}$ is the wave number, $\delta R = \overline{MA} - \overline{MB}$

the range difference, and γ is the angle between the target direction and the interferometer axis.

The estimate of γ is obtained from the $\Delta \phi_{AB}$ measurement:

$$\gamma = \arcsin \left(\frac{\Delta \phi_{AB}}{ka} \right) \tag{14}$$

This process can be easily implemented on a BSSS: the phase measurement is then taken between two identical receiving arrays, whose sections correspond to points A and B of Figure 5. The synchronous time series received on the two sensors are processed for a computation of their instantaneous phase difference (giving the arrival angle); together with the corresponding oblique distance given by the measurement time, this constitutes the raw bathymetric data.

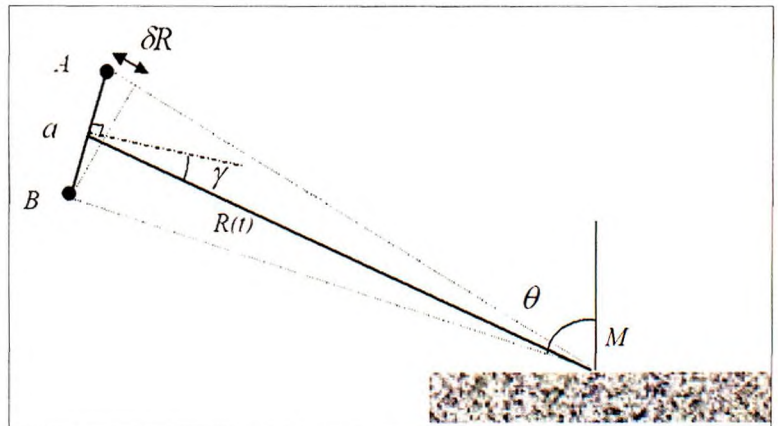


Figure 5: Interferometric angular measurement

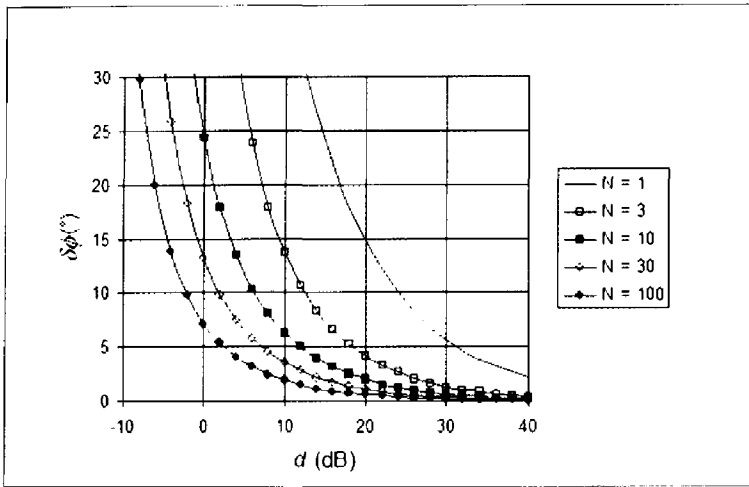


Figure 6: Phase difference standard deviation (in degrees) for a Rayleigh-fluctuating signal, as a function of signal-to-noise ratio (in dB), according to formulae (16) and (17). The curves are parameterised by the number N of samples used in the processing

The PDD method offers the advantage of not requiring a complex array structure in the vertical plane, and is often used for providing an auxiliary bathymetric function to sidescan sonars initially designed for imagery. As a counterpart to its simplicity it suffers from some disadvantages: ambiguity in the phase difference determination (13) leading to non-unique solutions to equation (14) and requiring special strategies for correction (see [Sintes, 2002]), and measurement degradation in the angular sector around the normal to the bottom (see below).

The interferometry angle error (disregarding here ambiguity problems for the phase difference) is directly a function of the phase measurement error $\delta\Delta\phi$ between the two receivers of the array; it is expressed from (13) taking into account, in γ the interferometer tilt angle:

$$\delta\theta_{PDD} = \frac{\delta\Delta\phi_{AB}}{2\pi} \frac{\lambda}{a} \frac{1}{\cos \gamma} \quad (15)$$

where λa is the angular aperture corresponding to the spacing a between the interferometer phase centres A and B .

For an individual time sample of the received signal (assumed noise-embedded and Rayleigh-fluctuating, see [Lurton, 2001]), the phase difference standard deviation $\delta\Delta\phi$ can be approached with a good precision by:

$$\delta\Delta\phi \approx 2 \left[\frac{12}{\pi^2} + d \right]^{-1/2} \left[1 - 0.05 \frac{d}{d+1} \ln d \right]^{-1} \quad (16)$$

The SNR d considered here should account for the three causes of noise discussed above and synthesised in (7).

Considering that practically the phase difference has to be obtained from processing a set of N samples ($N > 2$), it may be shown [Lurton, 2001] that its standard deviation $\delta\Delta\phi$ is given by:

$$\delta\Delta\phi \approx \left[\frac{1}{(N-1)d} + \frac{N}{2(N-1)(N-2)d^2} \right]^{1/2} \quad (17)$$

valid in the range of small phase fluctuations ($\delta\Delta\phi$ below 30°). It may be further approximated, in the limit of large values of d and N , by:

$$\delta\Delta\phi \rightarrow \left[\frac{1}{Nd} \right]^{1/2} \quad (18)$$

These formulae (17)(18) are illustrated in Figure 6, giving the phase difference standard deviation as a function of SNR and number of samples. More details and comparisons with numerical simulations are to be found in [Lurton01].

One gets from (1)(15) the depth measurement relative error:

$$\frac{\delta H_{PDD}}{H} = \frac{\delta\Delta\phi}{2\pi} \frac{\lambda \tan \theta}{a \cos \gamma} \quad (19)$$

where $\delta\Delta\phi$ is given by (17), in the usual case where several time samples are averaged.

It should be emphasised that for PDD processing, averaging over N samples is practically unavoidable, considering the noise suffered by the phase difference from a single sample; the price to be paid for this straightforward improvement is that the spatial resolution is then degraded proportionally to N .

Zero-phase Difference Instant

For this method which is a derivative of the previous one, a MBES receive array is partitioned into

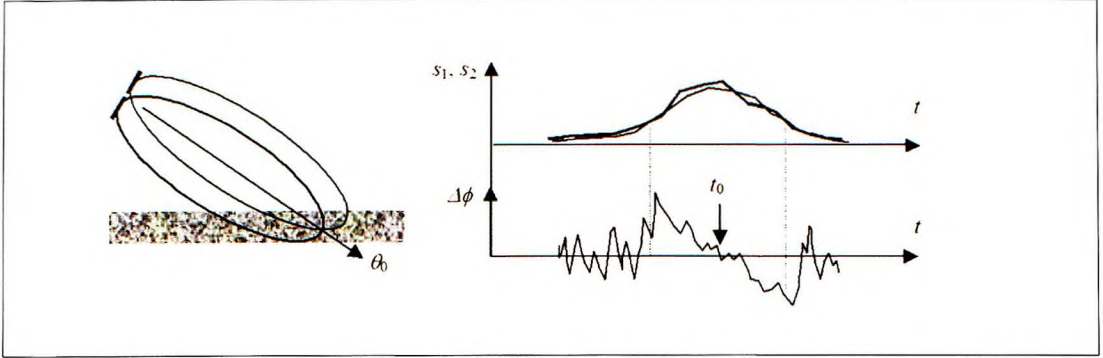


Figure 7: Measurement of the zero-phase difference instant: geometry of the half-beams associated with the two sub-arrays (left), envelope amplitudes of the temporal signals resulting from the two half-beams and measurement of the phase difference for determination of the instant t_0 of $\Delta\phi=0$ (right)

two sub-arrays. For a given receive direction, each sub-array forms a beam in the chosen direction. The phase difference is measured between the outputs of the two beams thus formed. The phase corresponding to the nominal direction of beams being compensated by beamforming, the zero-phase difference instant between the two signals corresponds to the arrival time of the signal according to the nominal steering angle.

The ZDI measurement makes it possible to reduce some of the constraints of the PDD method. Owing to the fact that the time signal is practically limited in extent by the sub-array aperture, the problems of phase ambiguities may be eliminated (depending on the sub-array lengths). The shifting footprint phenomenon can be minimised by accounting for the signal arrival direction, known *a priori* from beamforming. The ZDI gives however poor results close to the vertical. One will admit, in the following, that the method is only practically usable typically beyond 20° - 30° , and that the principal limitation of the performance is additive noise.

The performance of this measurement may be studied similarly to PDD, with some modifications. The phase difference variation is roughly linear around the instant t_0 of null-phase difference:

$$\Delta\phi(t) \approx ka \frac{c}{2} (t - t_0) \frac{\cos^2 \theta}{H \sin \theta} \quad (20)$$

The time measurement relative error around t_0 is then connected to the phase difference measurement error $\delta\Delta\phi$ (accounting that $H = \frac{ct}{2} \cos \theta$) by:

$$\frac{\delta t}{t} = \frac{\delta\Delta\phi}{ka} \tan \theta \quad (21)$$

When reported in the depth measurement relative error (1), this expression (21) becomes equivalent to equation (15) for the PDD angular measurement error along the interferometer axis ($\gamma=0$). The phase error term $\delta\Delta\phi$ depends on the output SNR for each sub-array. If the noise is dominated by the additive (external) component, the SNR to be considered is then

$$d = d_0 \beta \frac{4\pi\mu L w \cos \gamma}{\lambda^2} \quad (22)$$

d_0 being the physical SNR, β the degradation coefficient of the directivity index due to weighting, and μL ($\mu < 1$) the length of each sub-array; a is the interferometer spacing, i.e. the distance between the two sub-arrays centres; it is given by $a = L(1 - \mu)$.

The SNR is assumed to remain constant around the nominal direction of the considered beam. The standard deviation for the equivalent measurement of angle for ZDI is finally written:

$$\delta\theta_{ZDI} = \frac{\delta\Delta\phi}{2\pi} \frac{\lambda}{L(1 - \mu) \cos \gamma} \quad (23)$$

where $\delta\Delta\phi$ is given by (17). The depth relative error is finally:

$$\frac{\delta H_{ZDI}}{H} = \frac{\delta\Delta\phi}{2\pi} \frac{\lambda}{L(1 - \mu) \cos \gamma} \frac{\tan \theta}{\cos \gamma} \quad (24)$$

Practically, as in the case of PDD, a number of time samples have to be processed in order to estimate the zero-phase crossing, by fitting the measurement points with a linear or quadratic regression curve. While improving the precision of depth estimation, this unavoidably degrades its spatial resolution.

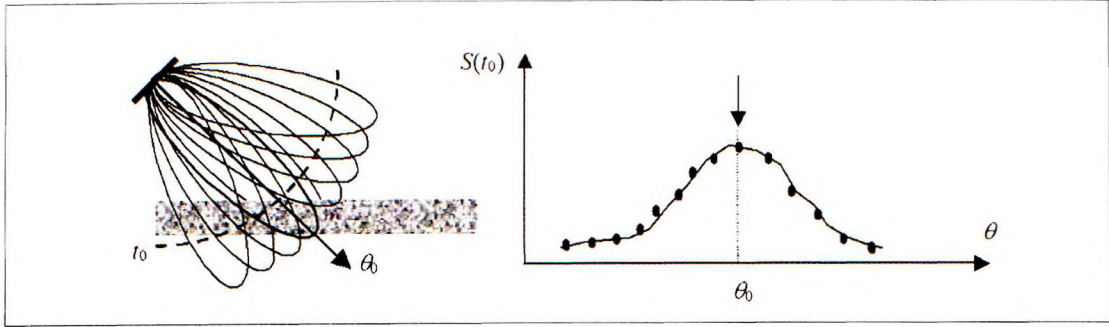


Figure 8: Measurement of maximum amplitude direction: a large number of beams are formed (left), and one detects at a given instant t_0 the level of maximum energy in the given angular direction θ_0 (right)

Maximum Amplitude Direction

This measurement method consists in estimating, at a given moment, the direction corresponding to the maximum energy received among a great number of beams formed with a small angular step (Figure 8).

The measurement quality is related to the actual processing used in angle estimation. Basically, it consists in searching for the angle with maximum amplitude in a series of fluctuating sample values corresponding to the outputs of the consecutive beams. So the performance will rather be, in the angle domain, similar to the one presented above for MAI in the time domain. At a given time the angle measurement error should be in:

$$\delta\theta_{MAD} = \frac{\xi\Omega}{\sqrt{N}} \tag{25}$$

where Ω is the lobe width considered in the estimation, and N is the number of angular points instantaneously available (Figure 8). The lobe width to consider is a combination of the array beamwidth $\Delta\theta$ from (8), and the angle spreading due to the signal length (10):

$$\Omega = \left[\Delta\theta_0^2 + \left(\frac{cT \cdot \cos^2 \theta}{2H \sin \theta} \right)^2 \right]^{1/2} \tag{26}$$

The depth measurement relative error is then formally identical to (12):

$$\frac{\delta H_{MAD}}{H} \approx \frac{\xi}{\sqrt{N}} \left[(\tan \theta \Delta\theta_0)^2 + \left(\frac{cT \cdot \cos \theta}{2H} \right)^2 \right]^{1/2} \tag{27}$$

Note that this accuracy corresponds to one given measurement instant; it may be improved further by averaging the angle estimation over a number of successive time samples (see below).

Based on the hypothesis that an instantaneous signal footprint may be considered as a point-like target, the MAD method is practically usable in configurations where the signal angular spreading at a given moment is not too penalising; this condition is well fulfilled in oblique incidence, but is not adequately satisfied close to the vertical.

Discussion

Variance Reduction Due to Averaging

A measurement corresponding to one single temporal sample is usually too disturbed and vague to be effectively usable; moreover the bathymetric profile thus carried out from a very dense set of temporal samples (typically the output sampling period is close to the signal duration itself) may be of little practical interest. A common practice is then to reduce the variance of individual measurements by taking into account N independent occurrences of each. The typical variation δX_N of a bathymetry measurement is given, at first approximation, by the standard deviation δX of each elementary measurement divided by \sqrt{N} ; however this improvement may be formally more complex, as it appears e.g. in eq.(17).

As a counterpart, increasing the number N of processed samples will cause a degradation in the resolution obtained: a given angle measurement will not be associated any more with a footprint on the bottom given by the only local and instantaneous resolution of the signal, but rather with a whole range extent defined by consecutive samples. Thus the final quality of measurement will depend on the number of points being used for averaging; this number will be limited by the homo-

generality of the bottom characteristics over the summation interval, and by the required resolution: a gain \sqrt{N} in precision, obtained by summing N samples, has to be balanced against a degradation of the horizontal resolution, approximately in $N/\sin\theta$. The number of samples used in the averaging filter can be selected in various ways. The relation between the time-sampling step (δt), and the variations in angle ($\delta\theta$) and x-coordinate (δx) is:

$$\delta x = \frac{2c\delta t}{c} \sin\theta = \frac{2H}{c} \frac{\sin\theta}{\cos^2\theta} \delta\theta \quad (28)$$

For a given sampling period δt , the corresponding δx increases for $\theta \rightarrow 0$, i.e. the resolution in x is degraded close to the vertical. On the other hand, for large values of θ , the resolution improves, but the measurement accuracy on depth z gets worse, as it appears in (1). Various strategies may be considered:

- Averaging over a number of samples N constant with range neither improves the resolution degradation at short distances, nor compensates in a sufficient way the precision degradation at long distances; the effect of this method is thus only to reduce by a global factor the total variance of the bathymetry measurement
- Averaging over a constant angular opening $\Delta\theta$ leads to a number of points increasing with range $N_{\Delta\theta} = \frac{2H}{c\delta x} \frac{\sin\theta}{\cos^2\theta} \Delta\theta$; this method

tends to compensate for the bathymetry error which increases with range, at the price however of a degraded resolution. This second solution is employed quite naturally in MBES, which usually provide only one sounding depth per beam, the footprint width of which (and therefore the number of available points) increases with the incidence angle. Practically, things are more complicated because of the necessary trade-off between the measurement precision (using as many samples as possible) and resolution (keeping N at a reasonable value). For instance in MAI measurement for steep-angle beams, with few samples available, the trend is to use the whole beam footprint data; at the other end, in actual ZDI processing, averaging is not to be made over the whole phase ramp, but rather over a restricted sector (smaller than the beam footprint) around the zero-phase crossing

- Finally, averaging over a constant interval Δx increases the number of samples with range, in

$N_{\Delta x} = \frac{2\Delta x}{c\delta x} \sin\theta$; this process imperfectly compensates for the degradation of precision in z , but can prove to be the most relevant strategy compared to the requirements of bathymetric mapping in order to try to maintain a constant horizontal resolution

Vertical Echoes

Bathymetry measurements near the normal to the bottom are prone to particular degradations, which are now examined. In the continuation, to keep simple notations and terminology, the normal to the bottom will be called 'vertical direction', with again the implicit assumption that the bottom is flat and horizontal. Several effects degrade the quality of the time-angle relation inside echo structure.

- Close to the vertical, in the absence of angular filtering by the directivity pattern, the instantaneous footprint of the signal is maximum in x , and is worth roughly:

$$\Delta x \approx H\theta \left[\left(1 + \frac{cT}{H\theta^2} \right)^{1/2} - 1 \right] \quad (29)$$

- The corresponding angular spreading (the angle sector covered instantaneously by the signal) is also maximum:

$$\Delta\theta = \theta \left[\left(1 + \frac{cT}{H\theta^2} \right)^{1/2} - 1 \right] \cos^2\theta \approx \theta \left[\left(1 + \frac{cT}{H\theta^2} \right)^{1/2} - 1 \right] \quad (30)$$

This instantaneous angular spreading effect is irreducible for systems without angular filtering (PDD) or carrying out an angular scanning at a given instant (MAD). On the other hand, for the two other modes of detection, processing data inside one formed beam, the angular spreading effect can be limited by the directivity lobe width, which fixes the upper limit of the $\Delta\theta$ value

- The footprint shift effect is also at its maximum; it is shown that its amplitude, depending on array mounting ψ , is then:

$$\delta x \approx \frac{a}{2} \cos\psi - H\theta + \sqrt{H^2\theta^2 + aH\sin\psi} \quad (31)$$

The corresponding SNR is given roughly by the ratio $\frac{\Delta x}{\delta x} - 1$ expressed from (29) and (31).

- The time-angle relation is smeared by specific physical effects already evoked in previously:

- seafloor roughness and sediment penetration
- Also it should be noted that the accuracy improvement obtained by ensemble averaging is of little effect then, due to the small number of available time samples in this angular sector
- The echo level is then at a very sharp maximum, due to the conjugation of the ensonified surface and backscattering strength. This can raise problems in processing by the receiver whose analogue electronics and A/D converter cannot accept such dynamics. In practice, gain control devices are implemented to avoid saturation related to this effect
- Close to the vertical, the signal fluctuations are especially strong, due to the ensonified surface extension, and to the sharp angular variations of backscattering strength in this zone. Moreover directivity patterns of the arrays used in sidescan sonars are often designed to lower the signal received from the vertical, in order to limit cross-talk between the two sides; their answer can also be disturbed by their mechanical environment, since they are usually mounted on towed fish sides; the resulting masking effect may cause phase disturbances in received signals.

All these combined effects preclude accurate interferometric measurements for geometries close to

a local surface normal. This is especially penalising for BSSS, lacking transverse resolution at these incidences; and to a lesser degree for interferometric MBES having the advantage of angular selectivity provided by narrow beams

Application Example

As an illustration of the above models, we consider here the case of a shallow-water multibeam echosounder, using MAI at steep incidences and ZDI at oblique grazing angles. The emitted level is 220 dB re.1 μ Pa at 1m, the nominal frequency is 100 kHz, with an absorption coefficient of 35 dB/km; the additive noise level is 45 dB re 1 μ Pa/ $\sqrt{\text{Hz}}$; the seafloor backscattering is given by a Lambert law with constant $BS_0 = -30$ dB re 1m²; the water depth is 50 m, and sound velocity 1500 m/s; the roughness amplitude considered in MAI is $h = 0.2$ m. Both arrays are rectangular and horizontally mounted. The transmitting array length is 0.75 m, and the beam is 1° wide; the receiving array dimensions are 0.50 and 0.20 m; beam-forming with a weighting factor $\alpha = 1.3$ leads to a beamwidth of 2°, increasing with the steering angle; the array gain is 36.5 dB, decreasing with steering angle. The signal duration is 0.5 ms, and the sampling frequency is 10 kHz. The sub-array size and interferometer spacing are given by

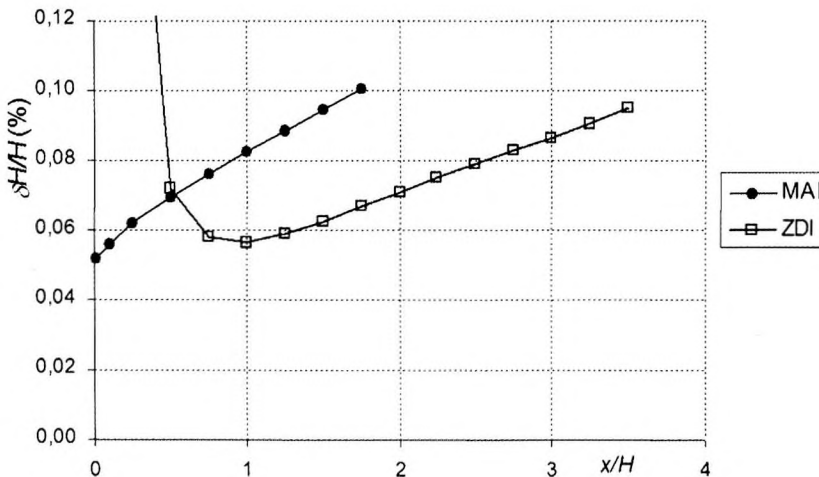


Figure 9: Relative depth error along a swath half-width (given by x/H , with $H=50$ m), for a 100-kHz multibeam echosounder using MAI and ZDI methods. See text for details

$\mu=0.5$; one half of the footprint points are used for ZDI estimation.

The model results are given in Figure 8. Most of the estimated depth error is smaller than 0.1 per cent, which is quite small but in good agreement with commonly observed performances of modern multibeam echosounders. This example makes clear the two regimes corresponding to the two bathymetry measurement methods. Close to the vertical the MAI error is low (around 0.04 per cent) and gently increases with incident angle; the ZDI is then unusable, but its accuracy improves as incident angle increases. The two methods give equal errors around 35° ($x/H \approx 0.7$), beyond which the phase detection gives better results; the ZDI error comes to a minimum around 45° ($x/H=1$), and increases regularly until a value of 0.1 per cent at 75° incidence ($x/H \approx 3.5$).

Conclusions

The acoustic measurement errors are often the less-well documented points in the various error-budget models available for sonar bathymetry performances ([Hare, 2002]). This is due on one hand to the fact that such analyses imply a thorough knowledge of the sonar characteristics, which may be difficult to obtain from the manufacturers; and on the other hand, the influence of other error cases (the main ones being the carrier's attitude measurement accuracy, and the compensation of the sound speed profile refraction) [Hare et al., 1995] can appear to be dominant in a number of cases. However, the need for estimating this category of acoustical measurement errors does exist, and will increase together with the system performance improvements and the users requirements. This paper aims at filling the lack in availability, for sonar users, of practical formulae modelling these effects.

We have proposed here accuracy models for the various methods of acoustic measurement used in bathymetric sonars, the purpose being to define formulations easily usable for performance prediction and experimental results analysis. This was done for the four methods currently used in modern bathymetry sonars. The proposed models explicitly feature on the one hand the geometrical parameters for the measurement configuration (water depths, incident angles) and the sonar arrays (dimensions, tilt angle), and on the other

hand the parameters of the emitted signal and its processing. They have been defined for an ideally flat homogeneous seafloor; specific effects such as seafloor type patchiness or sediment penetration have not been accounted for, despite their dominant influence in particular cases.

References

- D. Billon (1987) Bearing estimation of a single monochromatic plane wave with a linear receiving array in *Progress in Underwater Acoustics*, ed. H.M.Merklinger, Plenum Publishing Corporation, 1987
- W.S. Burdic (1984), *Underwater Sound System Analysis*, Prentice-Hall, Englewood Cliff, 1984
- J.G.Blackington (1986) *Bathymetric mapping with SeaMARC II: an elevation angle measuring side-scan sonar system*, PhD dissertation, University of Hawaii, 1989
- C. de Moustier (1988), *State of the art in swath bathymetry survey systems*, Int. Hydr. Rev., vol. 65, pp. 25-54, 1988
- C. de Moustier (1993), Signal processing for swath bathymetry and concurrent seafloor acoustic imaging, in *Acoustic signal processing for Ocean Exploration*, J. M. F. Moura and I. M. G. Lourtie, Eds.: NATO Advance Study Institute, pp. 329-354, 1993
- Ph. Denbigh (1989) *Swath bathymetry: principles of operation and an analysis of errors*, IEEE Journal of Oceanic Engineering, vol.14, No 4, pp 289-298, 1989
- E. L. Hamilton and R. T. Bachman (1982), *Sound velocity and related properties of marine sediments*, Journal of the Acoustical Society of America, vol. 72, pp 1891-1904, 1982
- R. Hare, A. Godin & L. Mayer (1995), *Accuracy estimation of Canadian swath (multibeam) and sweep (multi-transducer) sounding systems*, Canadian Hydrographic Service Internal Report, 1995
- R. Hare (2002), *Bathymetry error modelling: approaches, improvements and applications*,

Canadian Hydrographic Conference CHC 2002, Toronto, 2002

F.J. Harris (1978), *On the use of windows for harmonic analysis with the Discrete Fourier Transform*, Proc.IEEE, vol.66, N°1, pp51-83, 1978

G. Jin & D. Tang (1996), *Uncertainties of differential phase estimation associated with interferometric sonars*, IEEE Journal of Oceanic Engineering, vol.21, No 1, pp 53-63, 1996

F. Le Clerc (1994), *Performance of angle estimation methods applied to multibeam swath bathymetry*, Proc. IEEE Oceans'94, Brest, pp III 231-236, 1994

X. Lurton (2000), *Swath bathymetry using phase difference: theoretical analysis of acoustical measurement precision*, IEEE Journal of Oceanic Engineering 25(3), pp 351-363, 2000

X. Lurton (2001), *Précision de mesure des sonars bathymétriques en fonction du rapport signal/bruit*, Traitement du Signal, vol.18, n°3, pp 179-194, 2001

H. Maître (2001), *Traitement des images de RSO (SAR image processing)*, Hermes, Paris, 2001

F. Pohner (1987), *The Simrad EM100 multibeam echosounder, a new seabed mapping tool for the hydrographer*, 13th Int. Hydrographic Conf., Monaco, 1987

A.H. Quazi (1981), *An Overview of the Time Delay Estimate in Active and Passive systems for Target Localization*, IEEE Trans.Acoustics, Speech and Signal Processing, Vol.ASSP-29 N°3, pp527-533, 1981

V.Renard & J.P.Allenou (1979), *Le SeaBeam , sondeur multifaisceau du N/O Jean Charcot: descrip-*

tion, évaluation et premiers résultats, Int. Hydr. Rev., vol. 51, n° 1, pp 35-67, 1979

J.H. Satriano, L.C. Smith & J.T. Ambrose (1991), *Signal processing for wide swath bathymetric sonars*, Proc. IEEE Oceans'91, 1, pp 558-561, 1991

C. Sintès (2002), *Déconvolution bathymétrique d'images sonar latéral par des méthodes interférométriques et de traitement de l'image*, Ph.D dissertation, Université de Rennes 1, France, 2002

Biography

Xavier Lurton (born in Bordeaux, France, 1955; PhD of Applied Acoustics, 1979). He was for eight years (1981-89) with Thomson-Sintra ASM, mainly specialising in underwater sound propagation modelling for naval applications. In 1989 he joined IFREMER (the French oceanic research agency) in Brest as a R&D engineer. He worked on various acoustical oceanography applications (ocean tomography, telemetry, fisheries sonar) and managed the IFREMER acoustics laboratory for five years. He is now in charge of a technological research programme on advanced acoustical methods for seafloor characterisation, his current interests being both in physics of seabed backscattering, sonar signal processing and multibeam echosounder engineering. He has also been teaching underwater acoustics in engineering schools for several years, and he is the author of *An introduction to Underwater Acoustics* (Springer-Praxis, 2002). See review in this issue.

E-mail: lurton@ifremer.fr